Agronomy Research **14**(2), 485–494, 2016

Segmented capacitance sensor and first tests of inverse problem solution

J. Lev[1,*] and M. Wohlmuthová[2]

[1]Czech University of Life Sciences Prague, Faculty of Engineering, Department of Physics, Kamýcká 129, CZ 165 21 Prague 6, Czech Republic
[2]Czech University of Life Sciences Prague, Faculty of Engineering, Department of Mathematics, Kamýcká 129, CZ 165 21 Prague 6, Czech Republic
[*]Correspondence: jlev@tf.czu.cz

Abstract. The segmented capacitance sensor (SCS) is developed for the purpose of material throughput measurement. SCS can be used in precise agriculture (e.g. yield maps creation) or for controlling of mass flow in stationary lines. This sensor is a compromise between simple capacitance throughput sensor which has been developed at the Department of Agricultural Machines Faculty of Engineering of Czech University of Life Sciences Prague and electrical capacitance tomography sensor. The SCS consists of the bottom plate (bottom electrode) and several upper electrodes which are placed parallel above the bottom plate. The upper electrodes are sometimes called segments of an upper plate. The bottom plate is undivided and it is assumed that it will be stored under measured material. During the measurement process the electric capacitance between one upper electrode and the bottom plate is measured every time. The sensor should be able to determine the distribution of material between upper electrodes and the bottom plate. This paper presents the algorithm of inverse problem solution. The algorithm was tested in two phases. The testing during the first phase was done via mathematical model which was presented in previous papers. Results show that the presented algorithm can be used for the inverse problem solution. For the purpose of the second testing phase a simple SCS was made. Electrical capacitances were measured by precise LCR meter. In the second testing phase, the inverse problem algorithm was tested using the actually measured data.

Key words: finite element method, inverse problem, electrical capacitance tomography, electrical field.

INTRODUCTION

Material throughput measurement sensors are a very useful tool, both in the field of precision agriculture and other areas. This is noted by authors such as Kumhála et al. (2013) or Jadhav et al. (2014). Stafford et al. (1996), Savoie et al. (2002) and also Kumhála et al. (2009; 2010; 2013) have developed and tested different capacitance sensors for the material throughput measurement of plant material. The authors presented the advantages as: non-contact measurement, simple mounting on the machine, simplicity of the sensor, and low cost. The mentioned papers also confirmed the perspective of capacitance throughput sensors.

Kumhála et al. (2009) described the filling theory of the capacitance throughput sensor. It is very important that the capacitance of a sensor depends on the distribution

of material between its plates. Nevertheless, the simple capacitance throughput sensors cannot provide information about material distribution. This fact can produce significant errors. The problem can be resolved with an electrical capacitance tomography (ECT). ECT is based on multiple capacitance measurement of the sensing area. Usually ECT sensors are composed of 8–14 electrodes. This means that 28–120 independent capacitance measurements are obtained. The problem is that capacitance changes are very small and they have to be measured in a large range. For example Yang (2010) presents values of capacitance change between 0.1 fF to 0.1 pF. This author also suggests that measurement accuracy should be about 0.01 fF and better. It is evident that ECT sensors are very complicated devices and for some applications (e.g. throughput measurement) a simpler device can be used. An interesting possibility can be the segmented capacitance sensor (SCS). The idea of SCS has already been described in several papers e.g. Kumhála et al. (2012), Lev et al. (2013a; 2015). The SCS consists of the bottom plate (bottom electrode) and several upper electrodes that are placed parallel above the bottom plate. The upper electrodes are sometimes called segments of an upper plate. The number of measuring upper electrodes corresponds with the number of obtained signals. This is a fundamental difference from ECT sensors, which usually produce many more output signals. It is thus necessary to use a different approach towards the solution of the inverse problem.

Yang & Peng (2003) have compared the known methods of solving the inverse problem for ECT. This process the mentioned authors call 'image reconstruction'. The authors highlight a method based on the Landweber iteration that displays qualitatively the best results. This method was tested also on SCS by Lev et al. (2012). However, it has been shown that the SCS provides too few output signals for the use of this algorithm. It has also emerged that it is possible to determine relatively well the horizontal position of the sample in the imaging region, but the determination of the vertical position is very difficult. This is probably due to the spatial arrangement of SCS.

Algorithms used by ECT assume a completely random distribution of the material in the imaging area. However, in many applications it can be assumed that the examined material forms only the layer, which could be replaced by a polygonal line specifying the boundary between the material and the air. This paper tests the method of inverse problem solution based on this approach.

MATERIALS AND METHODS

For the purpose of the experiment there was assembled a testing SCS. The sensor had 8 measuring upper electrodes that were evenly spaced in the upper part of the frame. The distance between upper electrodes and the bottom plate was 100 mm, the sensing area was 360 mm in width and 400 mm in depth. Each measuring electrode was 40 mm wide and 400 mm long. Gaps between the upper electrodes were 5 mm. Dimensions of the bottom electrode were 360 mm in width and 400 mm in length. The frame of the sensor was made from phenolic paper sheet plate (Hp 2061). The thickness of the side walls was 20 mm and the thickness of the other parts was 10 mm. All electrodes (measuring upper electrodes and bottom plate) were made from material called cuprexit that was 1 mm thick. This material is used for printed circuit board (the laminate covered with a thin layer of copper).

For the measurement of electrical capacitance there was used precision LCR meter GW Instek LCR 8110G. Electrical capacitance was measured in each measuring procedure between an upper electrode and the bottom plate. Measuring upper electrodes that were not actually used for the measurements were connected to the earth wire. The frequency of the measuring circuit was set to 100 kHz.

Inverse problem algorithm

Plugging the measuring device creates in the scanned region of SCS a relative electric field. Providing the wavelength is significantly higher than the sensor dimensions the field can be described in 3D by the Laplace equation:

$$\nabla \cdot (\varepsilon_0 \varepsilon_r \nabla \varphi) = 0 \tag{1}$$

where: ε_0 – vacuum permittivity ($\varepsilon_0 = 8.85.10^{-12}$ Fm^{-1}); ε_r – relative permittivity (-); φ – electric potential (V).

The electric capacitance between the measuring electrode and a bottom plate is calculated by use of equation:

$$C = -\frac{1}{U}\int_{\Gamma} \varepsilon_0 \varepsilon_r \nabla \varphi \cdot \mathrm{d}\Gamma \tag{2}$$

where: C – electric capacitance between the measuring electrode and a bottom plate (F); U – voltage between measuring electrode and a bottom plate (V); Γ – area of the bottom plate (m^2); dΓ – normal vector to the infinitesimal segment of the bottom plate.

The mathematical 2D model developed on the bases of Eq. (1) has been in the past already verified several times (Lev et al., 2013a; 2013b; 2015). For the SCS inverse problem solution this mathematical model must be first created. In this paper, the finite element method was used employing the Agros2D 3.2 program. In this paper, the ordered n-tuple of real numbers $a_1, a_2, \ldots, a_n$ we will call (in sense of linear algebra) an n-component real vector a (vector a for short), $a = (a_1, a_2, \ldots, a_n)$. Further calculations follow the rules for algebraic vectors in vector space V_n. The input of the inverse problem algorithm is the vector of normalized capacitance changes. For each component it holds:

$$c_{ni} = (c_i - c_{0i})/(c_{maxi} - c_{0i}) \tag{3}$$

where: c_{ni} – the i-th component of the vector of normalized capacitance changes; c_i – electric capacitance between the i-th measuring upper electrode and a bottom plate; c_{0i} – electric capacitance between the i-th measuring upper electrode and a bottom plate when the sensor is empty; c_{maxi} – electric capacitance between the i-th measuring upper electrode and a bottom plate when the sensor is filled to its maximum (reference) capacity (i.e. the height of filling the SCS is 80 mm).

The algorithm aim is in finding a polygonal line, defined by points P_0 to P_9, such that it follows the actual material profile as close as possible. The end points P_0 and P_9 are during the evaluation process fixed at the edges of the sensing area. Points P_1 through P_8 are then located below centres of individual measuring upper electrodes. The problem

thus reduces to finding the values of points P_1 through P_8, i.e. the vector p. The value of each point is always an integer number defined as a ratio of the point distance from the bottom plate and the dimension of one square element of the mesh. The side of the square is 5 mm in length. The mesh scale is based on the compromise between the speed and the accuracy of calculations.

To avoid adjusting or newly creating the analysis mesh whenever manipulating with the polygonal line, the space in the sensing area, corresponding the maximum filling of the sensor, is subdivided into a rectangular mesh. The searched profile then does not eventually correspond to the polygonal line. Instead it is represented by squares for which it holds that at least 50% of their area is found below the polygonal line. An example of such a situation is shown in Fig. 1. The continuous grey line represents the actual outline of the material profile, the polygonal line is plotted in black and the resulting searched profile is displayed again in grey colour.

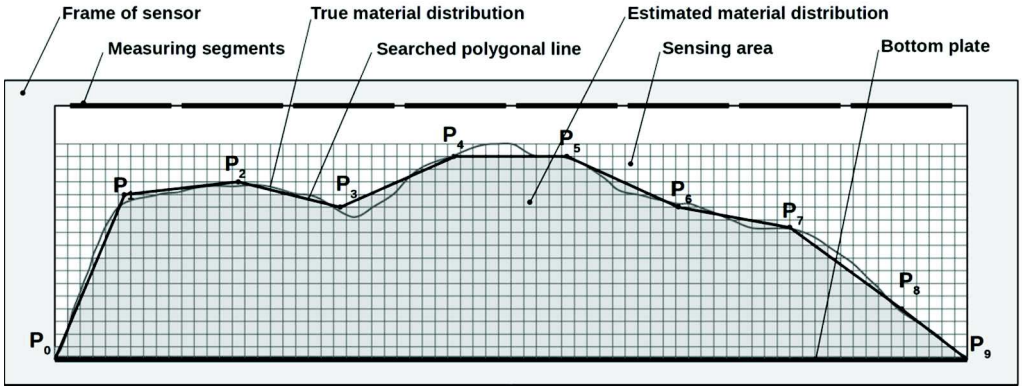

Figure 1. Cross-section of capacitance sensor. The actual distribution of the material, searched polygonal line and the estimated distribution of material are shown.

The following flowchart describes the algorithm:

1. Load vector of the normalized capacitance changes c_n, create vector p_j where index j represents the calculation step, choose the initial value of p_0 for $j = 0$.

2. Based on vector p_j define the distribution of material in the scanned region and for each of 8 measuring upper electrodes calculate with the help of Eq. (2) the electric capacitance between the measuring upper electrode and the bottom plate. Employing Eq. (3) calculated the normalized vector c_j (the values corresponding to an empty sensor and a sensor filled to its maximum capacity are also determined exploiting the mathematical model combined with Eq. (2)).

3. Calculate the coefficient ND_j defined as distance of vectors c_n and c_j

$$ND_j = \left\| c_n - c_j \right\| \tag{4}$$

4. Calculate the vector k, $k=(k_1,k_2,\ldots,k_i,\ldots)$, where

$$k_i = \frac{c_{ni} - c_{ji}}{\left| c_{ni} - c_{ji} \right|} \tag{5}$$

New vector p_{j+1}

$$p_{j+1} = f\left[p_j + k\right] \tag{6}$$

where f is a nonlinear function which defines individual coordinates of the vector:

$$\begin{aligned} x < 0 \quad &\Rightarrow f(x) = 0 \\ 0 \le x \le p_{max} \quad &\Rightarrow f(x) = x \\ x > p_{max} \quad &\Rightarrow f(x) = p_{max} \end{aligned} \tag{7}$$

where p_{max} is the maximum possible value of the vector coordinate. It corresponds to the height of the material outline in the scanned region having the sensor at its maximum capacity.

5. Check whether the new vector p_{j+1} (obtained through correction) has not already been used during the analysis. If not, the program returns with this new vector p_{j+1} to point 2 (index j is incremented by 1). Otherwise, the program continues.

6. Calculate the vector p_{j+1} again. First, determine the vector d_n where for each coordinate d_{ni} it holds

$$d_{ni} = \frac{c_{ni} - c_{ji}}{c_{ji}} \tag{8}$$

The vector p_j requires adjusting one component, which must correspond to the component in vector d_n with the largest absolute value and at the same time the following conditions must be satisfied

$$\left(d_{ni} < 0 \wedge p_{ji} > 0\right) \vee \left(d_{ni} > 0 \wedge p_{ji} < p_{max}\right) \tag{9}$$

The vector p_{j+1} is thus obtained from vector p_j such that the coordinate complying with the above described conditions is incremented by 1 if $d_{ni} > 0$ or reduced by 1 if $d_{ni} < 0$.

7. Perform operations described in point 2 with a new vector p_{j+1} and increment index j by 1.

8. Calculate the coefficient NDj using Eq. (4)

9. Compare the current and the previous coefficient ND. If $ND_j < ND_{j-1}$ continue with the next step 10. Otherwise, the searching process is terminated and the desired vector is identified with vector p_{j-1}.,

10. Based on vector cj determine a new vector pj+1 based on the procedure described in point 6. Then, return to point 7.

The experiment description

The inverse problem algorithm was tested on three different material profiles. As a material, timber prisms made from chipboard with a moisture content $MC_{w.b.} = 7.5\%$ were used. A relative permittivity was set equal to $\varepsilon_r = 4$ (James, 1975). First, the values corresponding to an empty sensor were measured. Then, eight tested prisms were placed longitudinally into the centre of the scanned region. These prisms created an object that was used as a reference filling of SCS. This object was 80 mm high, 360 mm wide and 220 mm long. It was accepted that such a region is maximally filled and the associated

measurement was used for normalizing other measurements. This reticular SCS is displayed in Fig. 2. Note the SCS cannot taken into account a different level of the filling in longitudinal direction. The depth of filling has to be constant all the time. Prisms from the same material were subsequently used to create three tested profiles. These are, including dimensions, shown in Fig. 3. Each measurement of electric capacitances was repeated three times.

Entirely identical scenario was simulated with the help of the Agros2D program. Distribution of the electric field corresponding to individual measurements was determined using the finite element method. The electric capacitance followed from Eq. (2). Initial value of vector p_0 was set to $p_0 = (8, 8, 8, 8, 8, 8, 8, 8)$. The inverse problem algorithm was also programmed in the environment of the Agros2D program. The programming language Python 2.7 and libraries NumPy 1.8.2 and Matplotlib 1.3.1 were exploited.

For the purposes of evaluating the results there was calculated the relative error of the calculated profile *RE*

$$RE = \frac{\|g_r - g\|}{\|g\|} \tag{10}$$

where g_r – vector of the contour of the calculated profile; g – vector of the contour of real profile.

The number of coordinates of vectors g_r and g equals the horizontal resolution of the sensing area. Each coordinate represents the height of the profile measured from the bottom plate. Another parameter that was used for the evaluation of the results was the relative error of profile area *REA*:

$$REA = \frac{a_r - a}{a} \tag{11}$$

where a_r – area of calculated profile (m^2); a – real area of profile (m^2).

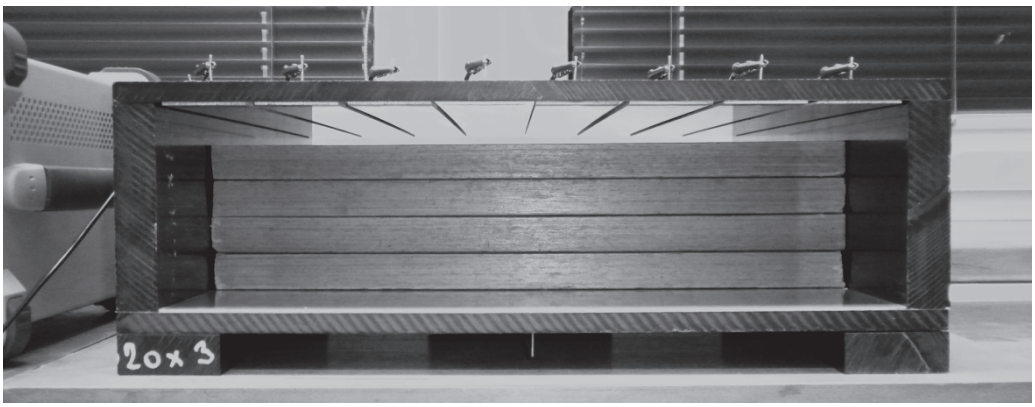

Figure 2. Reference filling of SCS with the testing material.

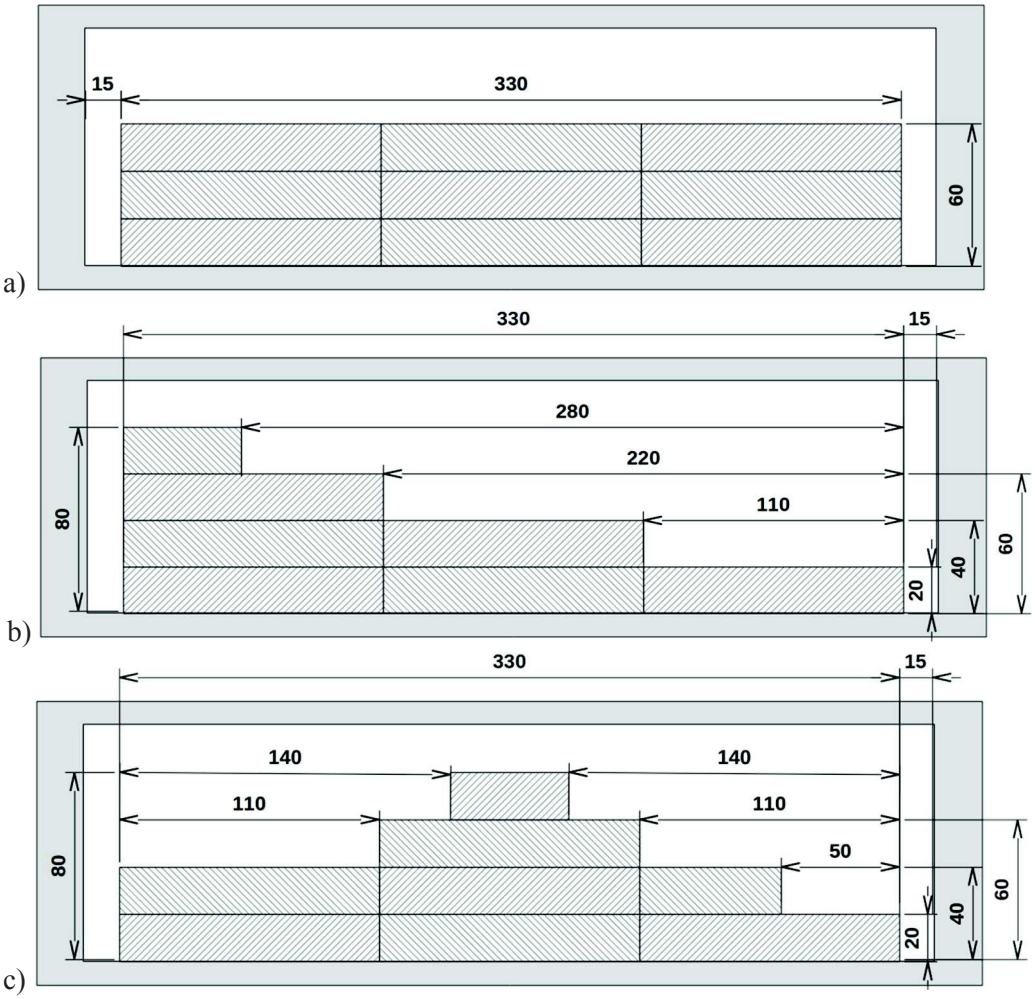

Figure 3. Profiles used for testing the inverse problem algorithm: a) – profile I, b) – profile II, c) – profile III.

RESULTS AND DISCUSSION

Results of the calculations are shown in Fig. 4. Figs 4 (a–c) represent the results based on real measurements. These results are therefore affected both by inaccuracies in the measurements and by the accuracy of the mathematical model that is used during the reconstruction. Figs 4 (d–f) represent the results calculated from simulations carried out in the program Agros2D. The effects mentioned in the text above could therefore not be applied here. So it can be assumed that the variations in Figs 4 (d–f) are due to the limits of the used algorithm.

From Fig. 4 it is apparent that the tested algorithm has problem to resolve the vertical walls of the test profiles. This behaviour is caused by using polyline which as a matter of principle cannot fulfil these requirements. However, the use of SCS is

planned rather for particular materials and chipboard prisms were chosen mainly because of the simple and clear definition of test profiles.

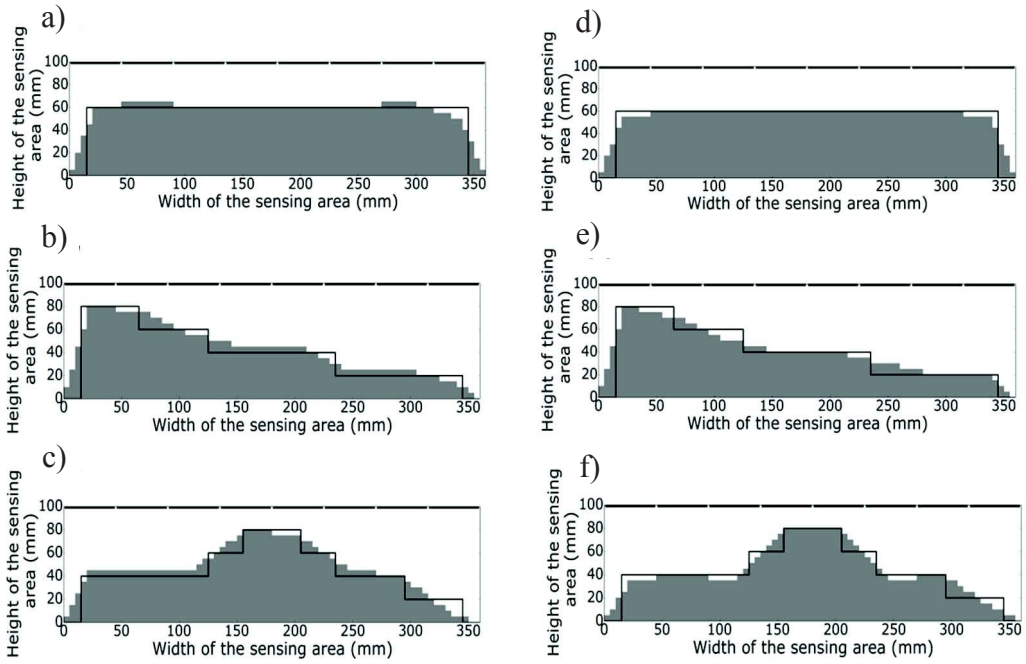

Figure 4. The calculated distribution of material in the SCS. Black curves show the actual distribution of test samples and the grey coloured area shows the calculated final layout. (a–c) represent the results based on real measurements, (d–f) represent the calculated results based on simulations carried out in the program Agros2D.

Table 1 contains calculated errors *RE* and *REA* for individual outcomes of the reconstruction algorithm. It can be said that in all three cases there was achieved a better result if the input data were obtained by simulation. This is an expected result. However, the differences posed against cases where the input data were actually measured, were not too large. It can therefore be concluded that the mathematical model used to describe the electric field in the sensing area of the SCS probably describes the actual behaviour of this electric field sufficiently.

Table 1. Comparison of results of the inverse problem algorithm. *RE* and *REA* error values are calculated by Eq. (10) and (11)

Variant	*RE* (-)	*REA* (-)
Profile I – measured input data	0.131	0.029
Profile I – calculated input data	0.119	0.008
Profile II – measured input data	0.193	0.081
Profile II – calculated input data	0.184	0.028
Profile III – measured input data	0.154	0.075
Profile III – calculated input data	0.135	0.005

RE error expresses the deviation between the actual and calculated shape of the profile. *RE* values in Table 1 range from 0.119 to 0.193. The lowest *RE* values were calculated for the profile I. It is probably due to the fact that it is a profile of the simplest shape. *REA* errors reflect the relative error of the profile area. This information may be useful if the SCS should be used for throughput measurement. According to Table 1 for cases where the input data were obtained by measurement, REA corresponds to the values 0.029 to 0.081, which is approximately 3–8%.

CONCLUSIONS

In this paper there was performed the first testing of algorithm for inverse problem solution at SCS. The results indicate that even for the relatively small number of output signals, it is possible to obtain valuable information on material distribution in the sensing area of the sensor. Further research is now needed to focus on the significant improving of the algorithm so that it can operate in real time.

ACKNOWLEDGEMENTS. This work was supported by the Internal Grant Agency of the Faculty of Engineering, Czech University of Life Sciences Prague (Project No. 2013:31160/1312/3114).

REFERENCES

Jadhav, U., Khot, L.R., Ehsani, R., Jagdale, V. & Schueller, J.K. 2014. Volumetric mass flow sensor for citrus mechanical harvesting machines. *Computers and Electronics in Agriculture* **101**, 93–101.

James, W.L. 1975. *Dielectric properties of wood and hardboard: variation with temperature, frequency, moisture content, and grain orientation.* Department of Agriculture, Forest Service, Forest Products Laboratory (U.S.), Madison, Wis, Res. Pap FPL 245, 32 pp.

Kumhála, F., Kavka, M. & Prošek, V. 2013. Capacitive throughput unit applied to stationary hop picking machine. *Computers and Electronics in Agriculture* **95**, 92–97.

Kumhála, F., Lev, J., Wohlmuthová, M. & Prošek, V. 2012. First tests with segmented capacitive throughput sensor. *Scientia Agriculturae Bohemica* **43**(1), 22–27.

Kumhála, F., Prošek, V. & Blahovec, J. 2009. Capacitive throughput sensor for sugarbeets and potatoes. *Biosystems Engineering* **102**(1), 36–43.

Kumhála, F., Prošek, V. & Kroulík, M. 2010. Capacitive sensor for chopped maize throughput measurement. *Computers and Electronics in Agriculture* **70**(1), 234–238.

Lev, J., Mayer, P., Wohlmuthová, M. & Prošek, V. 2013a. The mathematical model of experimental sensor for material distribution detecting on the conveyor. *Computing* **95**(suppl 1), 521–536.

Lev, J., Prošek, V., Wohlmuthová, M. & Kumhála, F. 2013b. The mathematical model of segmented capacitance sensor with grounded segments for determining of material distribution on the conveyor. *Agronomy Research* **11**(1), 73–80.

Lev, J., Prošek, V., Novák, P., Kumhála, F. & Wohlmuthová, M. 2015. Segmented Capacitance Sensor with Partially Released Inactive Segments. *Scientia Agriculturae Bohemica* **46**(3), 95 99.

Lev, J., Wohlmuthová, M. & Kumhála, F. 2012. Quality of material distribution imaging with segmental capacitive sensor using landweber's iterative algorithm. In: *Engineering for Rural Development 24.05.2012.* Latvia University of Agriculture, Jelgava, pp. 239–244.

Savoie, P., Lemire, P. & Thériault, R. 2002. Evaluation of five sensors to estimate mass-flow rate and moisture of grass in a forage harvester. *Applied Engineering in Agriculture* **18**(3), 389–397.

Stafford, J.V., Ambler, B., Lark, R.M. & Catt, J. 1996. Mapping and interpreting the yield variation in cereal crops. *Computers and Electronics in Agriculture* **14**, 101–119.

Yang, W.Q. & Peng L. 2003. Image reconstruction algorithms for electrical capacitance tomography. *Measurement Science and Technoogy* **14**, R1–R13.

Yang W.Q. 2010. Design of electrical capacitance tomography sensors. *Measurement Science and Technoogy* **21**(4), 1–13.